TU Delft

Delft University of Technology

Improving the computational efficiency of approximate gradients using a multiscale reservoir simulation framework

Jesus de Moraes, Rafael; Fonseca, Rahul; Helici, M.; Heemink, Arnold; Jansen, Jan Dirk

DOI
10.2118/182620-MS

Publication date
2017

Document Version
Final published version

Published in
SPE Reservoir Simulation Conference

Citation (APA)
Jesus de Moraes, R., Fonseca, R., Helici, M., Heemink, A., & Jansen, J. D. (2017). Improving the computational efficiency of approximate gradients using a multiscale reservoir simulation framework. In *SPE Reservoir Simulation Conference: Montgomery, Texas, USA* Article SPE-182620-MS SPE. https://doi.org/10.2118/182620-MS

Important note
To cite this publication, please use the final published version (if applicable).
Please check the document version above.

Copyright
Other than for strictly personal use, it is not permitted to download, forward or distribute the text or part of it, without the consent of the author(s) and/or copyright holder(s), unless the work is under an open content license such as Creative Commons.

Takedown policy
Please contact us and provide details if you believe this document breaches copyrights.
We will remove access to the work immediately and investigate your claim.

This work is downloaded from Delft University of Technology.
For technical reasons the number of authors shown on this cover page is limited to a maximum of 10.

Green Open Access added to TU Delft Institutional Repository

'You share, we take care!' – Taverne project

https://www.openaccess.nl/en/you-share-we-take-care

Otherwise as indicated in the copyright section: the publisher is the copyright holder of this work and the author uses the Dutch legislation to make this work public.

SPE-182620-MS

Improving the Computational Efficiency of Approximate Gradients Using a Multiscale Reservoir Simulation Framework

R. Moraes, TU Delft, Petrobras; R. M. Fonseca, TNO; M. Helici, A. W. Heemink, and J. D. Jansen, TU Delft

Copyright 2017, Society of Petroleum Engineers

This paper was prepared for presentation at the SPE Reservoir Simulation Conference held in Montgomery, TX, USA, 20–22 February 2017.

This paper was selected for presentation by an SPE program committee following review of information contained in an abstract submitted by the author(s). Contents of the paper have not been reviewed by the Society of Petroleum Engineers and are subject to correction by the author(s). The material does not necessarily reflect any position of the Society of Petroleum Engineers, its officers, or members. Electronic reproduction, distribution, or storage of any part of this paper without the written consent of the Society of Petroleum Engineers is prohibited. Permission to reproduce in print is restricted to an abstract of not more than 300 words; illustrations may not be copied. The abstract must contain conspicuous acknowledgment of SPE copyright.

Abstract

We present an efficient workflow that combines multiscale (MS) forward simulation and stochastic gradient computation - MS-StoSAG - for the optimization of well controls applied to waterflooding under geological uncertainty. The Iterative Multiscale Finite Volume (i-MSFV), a mass conservative reservoir simulation strategy, is employed as the forward simulation strategy. The i-MSFV method has the ability to accurately capture fine scale heterogeneities, and thus the fine scale physics of the problem. This allows for accurate and efficient simulations with fine-scale error estimates in a more computationally efficient coarse-scale simulation grid. The Stochastic Simplex Approximate Gradient (StoSAG) method, a stochastic gradient technique, inspired from Ensemble Optimization (EnOpt), is employed to compute the gradient of the objective function. Stochastic methods have recently been shown to be very efficient in terms of gradient quality and computational cost especially for robust optimization problems. They rely on the reservoir simulator as a black-box and perform a large number of forward simulations to approximate a gradient. In our numerical experiments, we investigate the impact of MS parameters such as coarsening ratio and heterogeneity contrast on the quality of the approximate MS-StoSAG gradient. Our experiments illustrate that i-MSFV simulations provide accurate forward simulation responses for the gradient computation, with the advantage of speeding up the workflow due to faster simulations. Speedups up to a factor of five on the forward simulation were achieved for the examples considered in the paper. The combination of speed and accuracy of MS forward simulation with the flexibility of the StoSAG technique (several different parameters/responses can be easily considered) allows for a flexible and efficient optimization strategy suitable for large-scale problems.

Introduction

We consider the life-cycle optimization of hydrocarbon production by manipulating well controls (pressure, rates or valve settings) for a given configuration of wells, a process also known as long-term production optimization or recovery optimization. In particular we consider robust optimization of strategies which maximize an objective function over an ensemble of reservoir model realizations to capture the effect of geologic uncertainty (Van Essen et al. 2009). The most efficient optimization tecniques for this purpose are gradient-based with gradients computed using the Adjoint method (Jansen 2011). However, the

implementation of an adjoint is time-consuming and requires access to the simulator source code. This has led to a growing popularity of stochastic gradient-based optimization techniques which are easy to implement and flexible to use with different control types as well as different reservoir simulators. One of the most used stochastic gradient-based techniques is Ensemble Optimization (EnOpt) which was first introduced by Chen et al. (2009). EnOpt uses a number of perturbed control vectors around a known control strategy where the number of perturbations is much lower than the total number of elements in the control vector (i.e. the number of well controls times the number of control time periods over the life time of the reservoir). The associated objective function values of these perturbed controls are used to approximate the gradient using linear regression.

For optimization of a single reservoir model, i.e. deterministic optimization, the computational effort to estimate the gradient increases with the number of perturbed controls to be evaluated. However, Chen et al. (2009) showed that for optimization over multiple reservoir models, i.e. for robust optimization, pairing one reservoir model to one perturbed control strategy leads to a similar computational efficiency as gradient-based techniques. Fonseca et al. (2014b) introduced an improved version of EnOpt for robust optimization, called Stochastic Simplex Approximate Gradient (StoSAG), which is theoretically more sound and produces higher- quality gradients. Moreover, they showed that, although the one-to-one pairing is computationally efficient, higher quality StoSAG gradients can be achieved by using a larger number of perturbations. Thus improving the computational efficiency of individual forward simulations, to allow for more perturbations, is the focus of this paper.

One of the ways to improve the computational efficiency of forward simulation models in optimization is the use of Reduced Order Models (ROM) (Cardoso et al. 2010; Jansen and Durlofsky 2016; van Doren et al. 2006). Alternatively, there, has been an increase in the applicability of different simulation strategies to speed up the computational process. One such technique is the Multiscale (MS) method (Hou and Wu 1997; Jenny et al. 2003). MS methods aim to solve the equations at a coarser scale, yet preserving the fine scale description. MS methods have increasingly been demonstrated as an efficient and accurate technique for reservoir simulation (Cusini et al. 2015; Kozlova et al. 2015, 2016; Tene et al. 2015). For an overview of important developments in MS we refer to Lie et al. (2016). Among these developments, an important one in the scope of the present work is the development of iterative MS methods, more specifically the Iterative Multiscale Finite Volume method (i-MSFV) (Hajibeygi et al. 2008; Hajibeygi and Jenny 2011). Due to the localization assumptions utilized in the construction of the MS basis functions, the solution obtained via an MS scheme is not as accurate as the fine-scale solution. However, these discrepancies can be resolved if an iterative scheme is employed. Moreover, because i-MSFV provides a fine-scale error estimate and an approximate, however fully conservative velocity field, it allows for both accurate and efficient simulation with control of the error estimate (Hajibeygi et al. 2012).

It is important to emphasize that, on one hand, MS methods provide approximate reservoir responses and stochastic methods, on the other hand, provide an approximation of the gradient. On that note, Krogstad et al. (2011); Moraes et al. (2016) show that analytical gradients (e.g. adjoint-based ones) computed via MS strategies provide an accurate enough approximations of the true gradient, capable of providing optimization results comparable to fine-scale optimizations. Also, Fonseca et al. (2015) provide a discussion on the quality of stochastic gradient compared to analytically computed ones.

The remainder of the paper is organized as follows. First, we discuss the StoSAG optimization methodology followed by the multiscale reservoir simulation framework which has been implemented in-house and used in this study. We then provide the workflow used for the optimization experiments performed in this paper. Following the theoretical descriptions of these two building blocks we illustrate the advantages and computational gains achieved on two different reservoir models for optimization cases with and without geological uncertainties.

Theoretical Framework

Stochastic Gradient Computation

In model-based optimization problems, traditionally, controllable variables, in individual wells or at field scale, such as injection or production rates, bottom-hole pressures (BHP) or ICV settings etc., are manipulated to maximize the value of an objective function such as Net Present Value (NPV) or Ultimate Recovery (UR). The controllable variables commonly referred to as controls and denoted by the vector $\mathbf{u}$ consist of all the variables to be optimized at the different control time steps. In this section we briefly outline the StoSAG method first introduced in Fonseca et al. (2014b) which is a modified version of the ensemble optimization method first introduced by Chen et al. (2009). For a detailed description of the methodology we refer to Fonseca et al. (2016).

For a control vector $\mathbf{u}^{\ell}$ we generate an ensemble of multi-variate Gaussian distributed perturbed control vectors $\{\mathbf{u}_1, \mathbf{u}_2, \ldots\ldots, \mathbf{u}_M\}$, around the control vector $\mathbf{u}^{\ell}$ with a user defined covariance matrix $\mathbf{C}$, where ℓ is the optimization iteration index. At the first iteration the choice of the control vector is user-defined and at subsequent iterations determined by the optimization algorithm. The covariance matrix $\mathbf{C}$ is usually kept constant throughout the optimization although methods exists to adaptively update the covariance matrix see e.g. Fonseca et al. (2014a); Stordal et al. (2016). The objective function J chosen to be optimized is then evaluated for each of the perturbed control vectors $\{\mathbf{u}_1, \mathbf{u}_2, \ldots\ldots, \mathbf{u}_M\}$ which leads to a corresponding set of objective function values $\{J_1, J_2, \ldots\ldots, J_M\}$.

To estimate the stochastic gradient we assemble a mean-shifted matrix of the control vectors $\mathbf{U}$ defined as

$$\mathbf{U} = [\mathbf{u}_1 - \mathbf{u}^{\ell} \quad \mathbf{u}_2 - \mathbf{u}^{\ell} \cdots \mathbf{u}_M - \mathbf{u}^{\ell}], \tag{1}$$

and a mean-shifted vector of the corresponding objective function values $\mathbf{j}$ defined as

$$\mathbf{j} = [J(\mathbf{u}_1) - J(\mathbf{u}^{\ell}) \quad J(\mathbf{u}_2) - J(\mathbf{u}^{\ell}) \cdots J(\mathbf{u}_M) - J(\mathbf{u}^{\ell})]^T. \tag{2}$$

The equations described above can be used for deterministic (single geological model) optimization. Recently many papers have investigated the theoretical and practical applications of stochastic gradients for robust optimization; see e.g. Chen (2008); Fonseca et al. (2014b) and references therein. In this paper we use a 1:1 ratio, i.e. one reservoir model to one perturbed control strategy, to robustly estimate the gradient. This leads to a slightly different notation for the vector of objective function anomalies given in (2) which for robust optimization is defined as

$$\mathbf{j} = [J(\mathbf{u}_1, \mathbf{m}_1) - J(\mathbf{u}^{\ell}, \mathbf{m}_1) \quad J(\mathbf{u}_2, \mathbf{m}_2) - J(\mathbf{u}^{\ell}, \mathbf{m}_2) \cdots J(\mathbf{u}_M, \mathbf{m}_M) - J(\mathbf{u}^{\ell}, \mathbf{m}_M)]^T. \tag{3}$$

where m are the geological model realizations which are equal in number to the number of perturbed control vectors. The StoSAG gradient is then calculated with linear regression and is given by (Fonseca et al. 2016)

$$\mathbf{g} = (\mathbf{U}(\mathbf{U}^T))^{+}\mathbf{U}\mathbf{j}, \tag{4}$$

where the superscript + indicates the Moore-Penrose pseudo inverse. The gradient $\mathbf{g}$ calculated above is then utilized in a simple steepest ascent algorithm (Nocedal and Wright 2006) to calculate an updated control vector until convergence is achieved. Do and Reynolds (2013) have shown that the formulation provided above has many commonalities with other stochastic gradient methods such as Simultaneous Perturbation Stochastic Approximation (SPSA) (Spall 1992).

Multiscale Reservoir Simulation

Multiscale (MS) methods (Hou and Wu 1997; Jenny et al. 2003), in summary, use locally constructed MS basis functions to enable the solution of the original fine-scale problem in a coarse scale and allow the solution to be accurately represented back to the fine-scale representation of the reservoir model.

In the context of this work we consider an immiscible, incompressible two-phase flow regime. Because MS methods are well-suited to solve elliptic problems, a sequential strategy to solve the governing equations is traditionally considered. Here, an Implicit in Pressure, Explicit in Saturation (IMPES) coupling is employed. For further explanations about the governing equations and solution strategies see, e.g., Aziz and Settari (1979).

In our simulator the flow (pressure) equation, is solved via the Multiscale Finite Volume (MSFV) method. The MSFV method, by construction, is mass conservative (Jenny et al. 2003). This is achieved via the introduction of basis functions, which are local solutions to the governing flow equation, subject to assumed local boundary conditions, without right-hand-side (RHS) terms

$$-\nabla \cdot (\lambda \cdot \nabla \varphi) = 0, \tag{5}$$

where λ is the mobility and φ is the basis function value. These local basis functions construct the prolongation (interpolation) operator, which is responsible to map (interpolate) the coarse-scale solution to fine-scale resolution (Wang et al. 2014; Zhou and Tchelepi 2012). This involves the definition of a primal coarse grid (on which the conservative coarse-scale system is constructed) and a dual coarse grid, which is obtained by connecting coarse nodes. Coarse node is a fine cell inside (typically at the center) each coarse cell. Basis functions are solved locally on these dual coarse cells. Such overlapping coarse and dual coarse grids are crucial for conservative solutions in MSFV. An illustration of the MSFV grids is provided in Fig. 1.

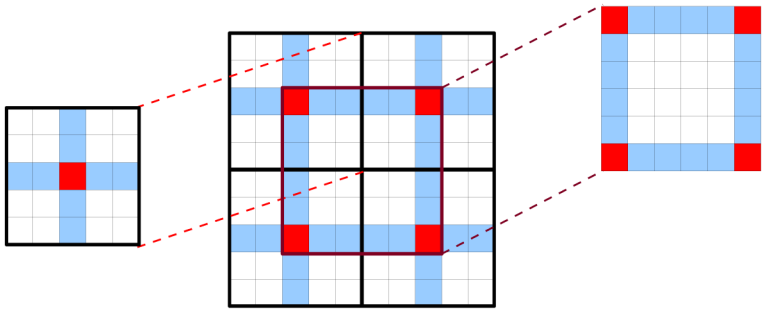

Figure 1—Illustration of MSFV coarse grids for a 2D domain. Given a fine-scale grid (shown in light solid black lines), the coarse grid (shown in solid bold black) is imposed as a non-overlapping partition of the computational domain. The coarse nodes (vertices) are then selected (filled in red cells). Connecting coarse nodes constructs the dual-coarse grid (highlighted in blue) where basis functions are solved.

As basis functions do not account for RHS terms, wells terms are considered as supplementary functions, called well functions (Jenny and Lunati 2009). Well functions are local solution of the flow problem considering unity solution at the well (i.e., $p_w = 1$). An illustration of basis and well functions is provided in Fig. 2. The prolongation operator can be expressed in terms of the basis functions corresponding to each coarse cell $j = 1,\ldots, N_C$ and each well function ψ_w corresponding to all $w = 1,\ldots,N_w$ wells adds a column vector to the porous rock prolongation operator

$$\mathbf{P} = \left[\begin{array}{ccc|ccc} \varphi_1 & \cdots & \varphi_{N_C} & \psi_1 & \cdots & \psi_{N_W} \end{array} \right]. \tag{6}$$

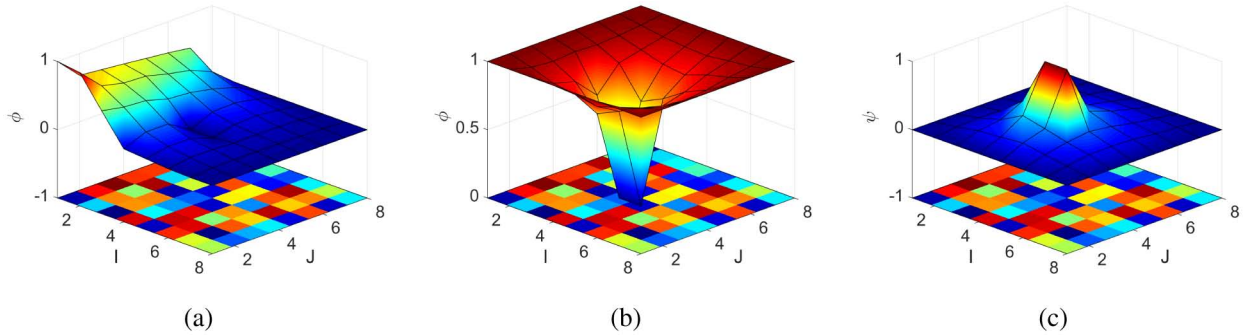

Figure 2—(a) Basis function, (b) sum of all basis functions and (c) well function for a given heterogeneous porous media (represented in the bottom of the plots) in a given dual-grid cell containing a well (source term). The well perforates two fine grid blocks in the center of the dual grid block.

The computation of well/basis functions are only performed once in the simulation, as a pre-processing step. During the multiphase run, they are adaptively updated only where the local properties within the specific dual cell is changed (Jenny et al. 2005). It is clear that the computation of basis functions is highly parallelizable, an advantage with respect to global-based ROM approaches.

The MS system can then be algebraically expressed as (Wang et al. 2014)

$$(\mathbf{RAP})\,\check{\mathbf{p}} = (\mathbf{Rq}) \tag{7}$$

where **R** is the restriction based on a finite volume integration operator at coarse scale resulting on a matrix of 0's and 1's (see e.g. Wang et al. (2014)). The interpolated fine-scale pressure is obtained by

$$\mathbf{p}' = \mathbf{P}\check{\mathbf{p}}. \tag{8}$$

Due to the localization assumptions utilized to compute the basis functions, the pressure solution obtained via a MSFV simulation is not as accurate as the fine scale solution. However, these discrepancies can be resolved if an iterative scheme is employed (Hajibeygi and Jenny 2011). The Iterative Multiscale Finite Volume method (i-MSFV) is capable of resolving these differences by resolving the high frequency errors via some iterative solve iterations (smoothing) in the fine scale and resolving the low frequency errors via the MSFV coarse scale solution. In brief, the method consists of re-writing Eqs. (7) and (8) in residual form and to iteratively solve the resulting system of equations until a convergence criterion is met. Note that i-MSFV delivers conservative coarse-scale solutions after any iteration stage. As such, it is not used as a linear solver, but to maintain the desired user-defined accuracy.

Following the MS pressure equation solution, we solve for the saturations at the fine scale. Because of the hyperbolic nature of the transport equations, fine grid scale resolution is necessary in order to capture the local, sharp saturation fronts. However, although the MSFV approximated solution is, by design, conservative at the coarse scale, it is not conservative at the fine scale. There different alternatives to build a fine-scale conservative velocity field to be used in the solution of the transport equation in fine scale. One option is to solve additional local Neumann problems at the primal-coarse grid domains (Jenny et al. 2005). Note that such a reconstruction stage should be done only for those coarse cells where the transport equation is needed to be solved at the fine- scale. Alternatively, one can smooth the fine-scale i-MSFV solution until a sufficiently small fine-scale residual is achieved. Like the former, this conservative velocity field reconstruction can also be done adaptively (Hajibeygi et al. 2012), with the additional advantage of controlling the solution quality via an error estimate.

Another important aspect associated with MS multiphase simulations is that basis functions from previous time steps can be stored and reused for most of the local domains in the next time step. Only for those local domains where mobility changes fall beyond a threshold value the basis functions need to be updated. Such an adaptive strategy can be employed for i-MSFV as well, i.e., the iterative procedure (smoothing stage)

can be employed only where and when the residual norm falls beyond a threshold value (Hajibeygi and Jenny 2011).

Finally, because CourantFriedrichsLewy (CFL) conditions for numerical stability (Coats et al. 2003) can be very restrictive in terms of the time-step size selection, we employ an asynchronous time-stepping strategy (Chen et al. 2004). This is achieved by solving the transport equation using small time-steps, hence honoring the CFL condition, but keeping pressure and velocity fields unchanged.

MS-StoSAG workflow

In this paper we have used the workflow presented in Fig. 3 for our optimization experiments. Note that the evaluation of the model responses is performed via MS reservoir simulation as a means to improve the computational efficiency of our optimization workflow. Although a simple steepest-ascent with variable step size optimization algorithm has been used, the framework is flexible to allow the use of more sophisticated ones.

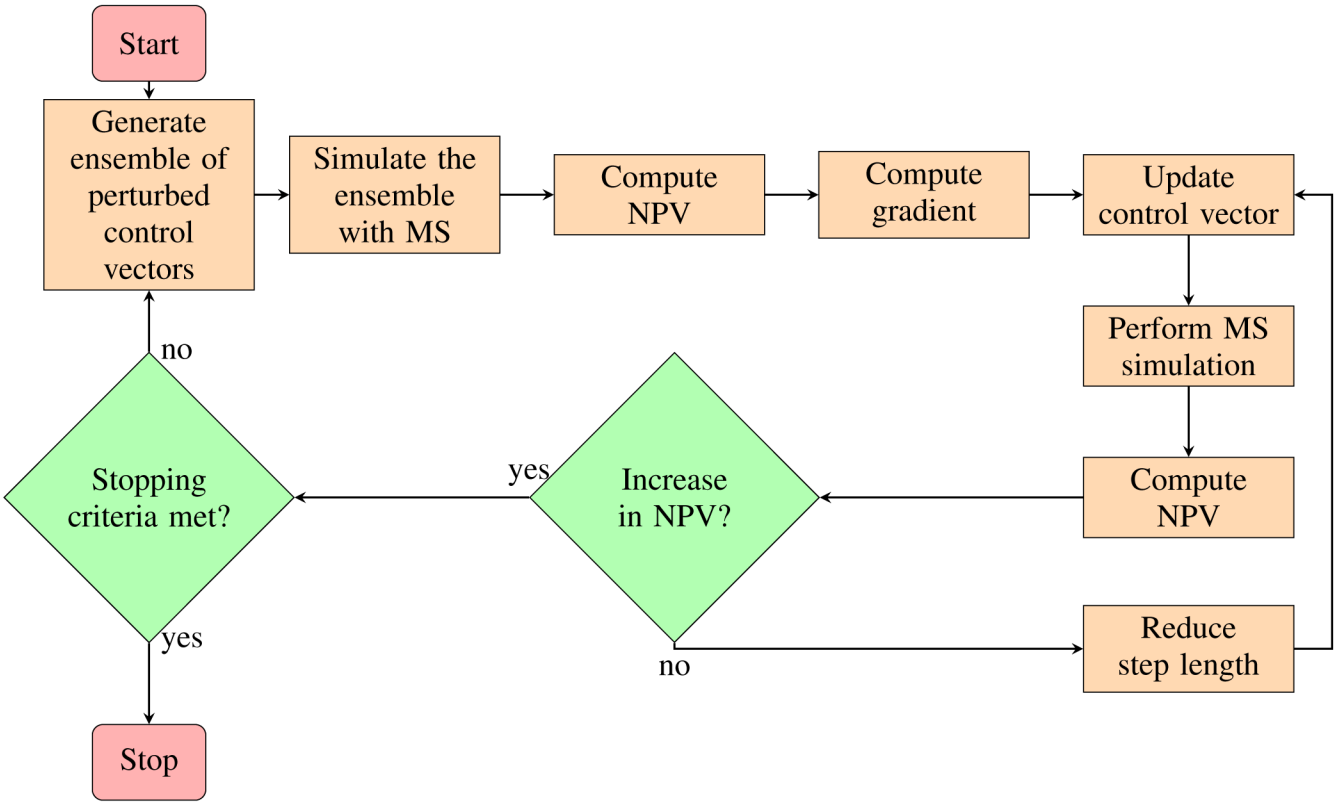

Figure 3—The MS-StoSAG optimization workflow. MS reservoir simulation is used in the evaluation of the model responses.

An in-house, research-oriented MS reservoir simulator is used for the purpose of the experiments. The simulator has been developed based on the theoretical framework here described. It has been benchmarked to other research simulators like MRST (Lie et al. 2012). An overview of the MS reservoir simulator can be found in Fig. 4. In the workflow, the tolerance E controls the reconstruction of the basis functions (BF), which only happens when a given error metric e exceeds the tolerance. The transport solver time-step Δt_s is limited by CFL conditions, but the flow solver time-step Δt_p is not. The velocity field is kept unchanged until the transport solver time t_s reaches Δt_p. The simulator outputs the information required to compute the gradient and objective function when the final time t_f is reached.

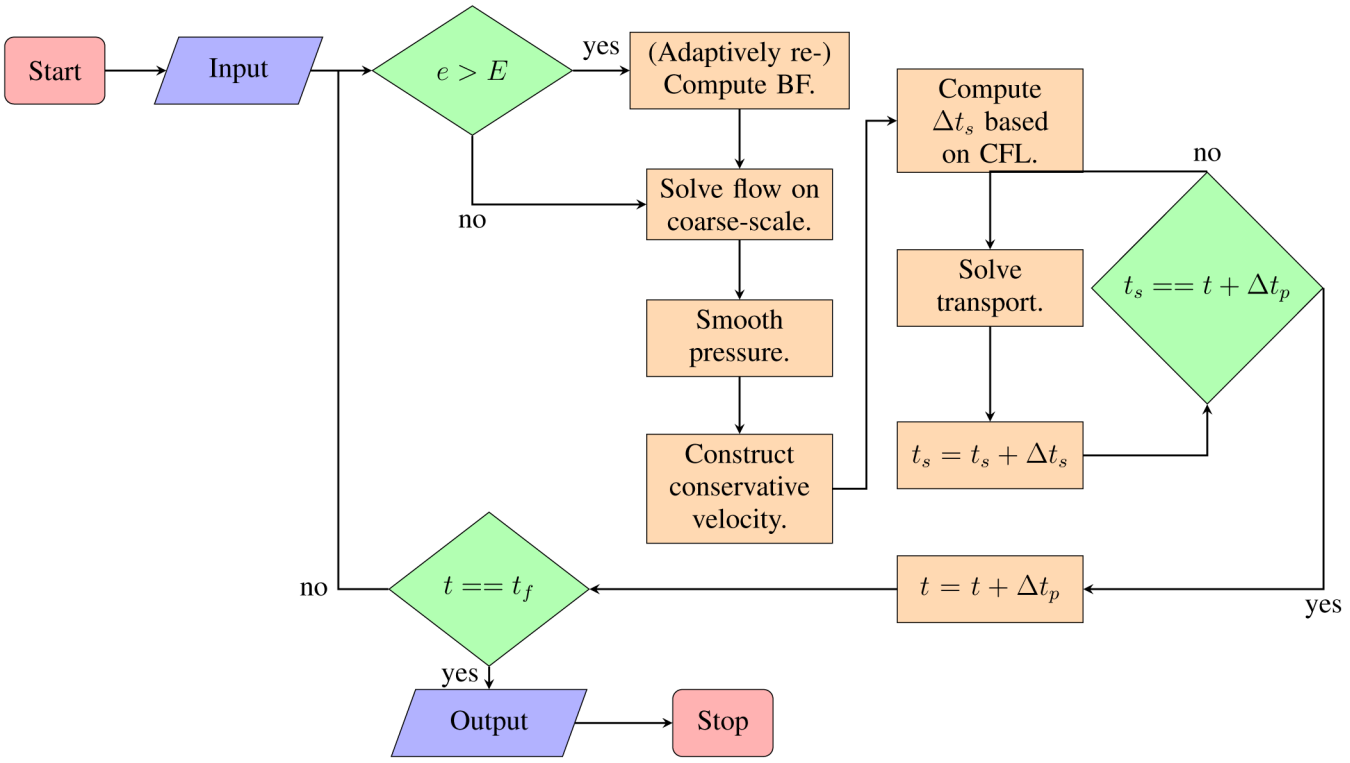

Figure 4—Schematic description of the MS reservoir simulation.

Numerical Experiments

We illustrate the application of our proposed framework in the life-cycle optimization of two different models. For both models, the controls are bottom-hole pressures in the injection and production wells. The objective function used for optimization is a standard economic objective, Net Present Value (NPV), as defined in Eq. (9), for which we use the prices provided in Table 1.

$$J = \sum_{k=1}^{K} \frac{[(q_{o,k}) \cdot r_o - (q_{wp,k}) \cdot r_{wp} - (q_{wi,k}) \cdot r_{wi}] \cdot \Delta t_k}{(1+b)^{\frac{t_k}{\tau_t}}} \tag{9}$$

Table 1—Costs associated with oil production.

	Value	Unit
Oil price	252	\$/m^3
Cost of injected water	60	\$/m^3
Cost of produced water	30	\$/m^3

where $q_{o,\,k}$ represents the oil production rate in m^3/day, $q_{\mathrm{wp,\,k}}$ is the water production rate in m^3/day, $q_{wi,\,k}$ is the water injection rate in m^3/day, r_o is the price of oil produced in \$/m^3, r_{wp} is the cost of produced water in \$/m^3, r_{wi} is the cost of injected water in \$/m^3, Δt_k is the difference between consecutive time steps in days, b is the discount factor expressed as a fraction per year, t_k is the cumulative time in days corresponding to time step k, and τ_t is the reference time period for discounting, typically one year.

In the MS simulation of all numerical experiments there is no basis function reconstruction. Instead, we delegate the resolution of the discrepancies left by the localization assumptions and inaccuracies due to outdated basis functions to the i-MSFV smoothing step. Also, the conservative velocity field is reconstructed

directly from the smoothed pressure field. For such, we require the i-MSFV loop to reduce the the fine scale residual in one order of magnitude, and the fine scale residual tolerance after smoothing is set to 10^{-6}. A l^2-norm is employed to computed the residual norm. The stabilized bi-conjugate gradient iterative solver with ILUT preconditioner (Saad 1994) is used as fine-scale smoother.

Five-Spot Model

In the first numerical experiment, a simple synthetic 2D inverted five-spot model is considered. It consists of a 21 × 21 regular mesh with grid block size dimensions of 33.3 × 33.3 × 2 m. The reservoir porosity is constant and equal to 0.3. The permeability distribution is depicted in Fig. 5 and the fluid properties are described in Table 2. For the optimization, we have 5 control variables per control time step. In this exercise we use 6 control time steps of 720 days each, thus we optimize 30 variables. The values of the bottom-hole pressures are bounded for the production wells between a minimum value of 280 bar and a maximum value of 300 bar. The injection well pressures are bounded between a minimum value of 300 bar and maximum value of 320 bar.

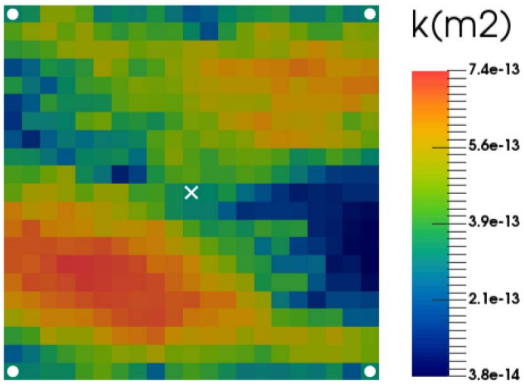

Figure 5—The permeability realization used for deterministic optimization and well placement

Table 2—Fluid properties for five-spot Model.

Property	Value	Unit
Oil dynamic viscosity (μ_o)	0.5×10^{-3}	Pa s
Water dynamic viscosity (μ_w)	1.0×10^{-3}	Pa s
End-point relative permeability, oil (k_{row})	0.9	-
End-point relative permeability, water (k_{rw})	0.6	-
Corey exponent, oil (N_o)	2.0	-
Corey exponent, water (N_w)	2.0	-
Residual-oil saturation ($S_{or} = 0.2$)	0.2	-
Connate-water saturation (S_wc)	0.0	-

Deterministic Life-cycle Optimization. We first consider a single model realization. For this purpose we use an ensemble of 50 perturbed control vectors with a perturbation size defined as 10% of the difference between the min and max bounds of the controls. The stopping criteria used is a maximum number of 25 optimization iterations. The initial starting strategy is one wherein the injector well operates at a constant BHP of 310 bars and the production wells at a constant BHP of 290 bars. When working with reduced order or upscaled models it is imperative to compare and validate the results with respect to the fine scale model realization. Fully Implicit methods (FIM) are commonly used for reservoir simulation. In the appendix we compare the differences in performances between FIM and IMPES on the fine scale model. We observe that

higher objective function values are achieved when using the IMPES soultion strategy. The MS reservoir simulator used here is based on the IMPES coupling and thus in the remainder of this paper we will compare our multiscale model results to the fine scale model run with IMPES.

Multiscale Optimization. We consider two different coarsening ratios to test the efficiency of our proposed MS-StoSAG workflow. The two coarsening ratios are 7x7 and 3x3. Thus a deterministic optimization with the optimization parameters discussed above is performed for 3 different models, fine scale using IMPES, i-MSFV 7x7 and i-MSFV 3x3. The optimization process is illustrated in Fig. 6. We observe that all three models find optimal strategies which produces approximately similar NPV values. We also observe that while the i-MSFV 7x7 model achieves a slightly lower NPV compared to the fine scale IMPES model, the i-MSFV 3x3 model achieves a higher NPV than the other two models. Thus the coarsest model used produced the highest NPV which may be counter-intuitive. Cross validation of the i-MSFV strategies on the 21x21 fine scale model produces NPV values which are indistinguishable from each other which could be the result of a relatively simple small model. Fig. 7 is a comparison of the optimal control strategies obtained from the different models. We observe that all the strategies are very similar to each other thus the objective function values are also similar. A speedup of approximately factor four was achieved with details discussed in the computational efficiency section discussed below.

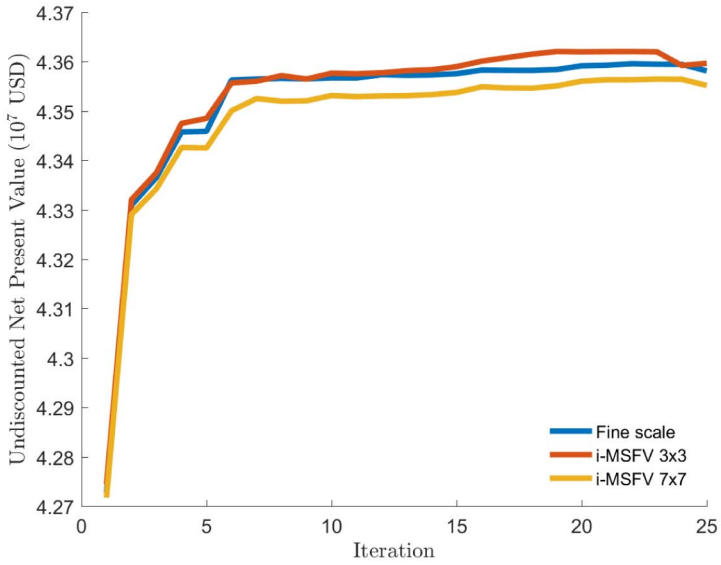

Figure 6—Comparison of the objective function through the iteration process for IMPES and the two i-MSFV models

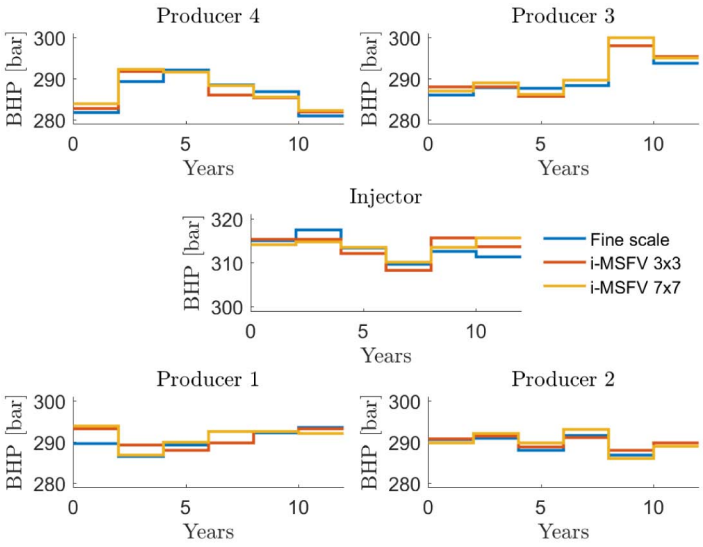

Figure 7—Comparison of the optimal control strategies between IMPES and two -MSFV models

Sensitivity to Optimization Parameters. The parameters which influence the computation of a stochastic gradient such as ensemble size of perturbed controls, perturbation sizes to generate the ensemble of controls, random seeds used to generate the perturbed controls were varied and tested with the different i-MSFV models. The results from this exercise followed the exact same trends as reported in earlier publications see e.g. Fonseca et al. (2015) who investigated the impact of gradient quality based on the various parameter choices.

Robust Life-cycle Optimization. Inclusion of uncertainty within the optimization framework is usually accounted for by utilizing an ensemble of equiprobable geological model realizations. In this paper a large ensemble of 1,000 realizations of the five-spot model was generated via the decomposition of a reference permeability image using Principal Component Analysis parameterization. See Jansen (2013) for more details. Fig. 8 illustrates 4 different permeability realizations from a reduced ensemble of 50 members used in the optimization experiments. The reduced ensemble was selected by simulating all 1000 realizations with the same control vector and uniformly sampling realizations based on the highest, lowest and intermediate objective function values. We acknowledge that there exists a range of formal clustering techniques to carefully select a representative ensemble. For the proof-of-concept optimization experiments in this paper the representativeness of the selected ensemble to a larger ensemble is deemed to be outside the scope of this paper. Building basis functions is a key element in the multiscale simulation framework. For the robust optimization experiments considered in this paper the basis functions for every single geological model realization have been built. Innovative techniques to use a limited number of basis functions in order to improve the computational efficiency of the optimization framework are outside the scope of the current paper.

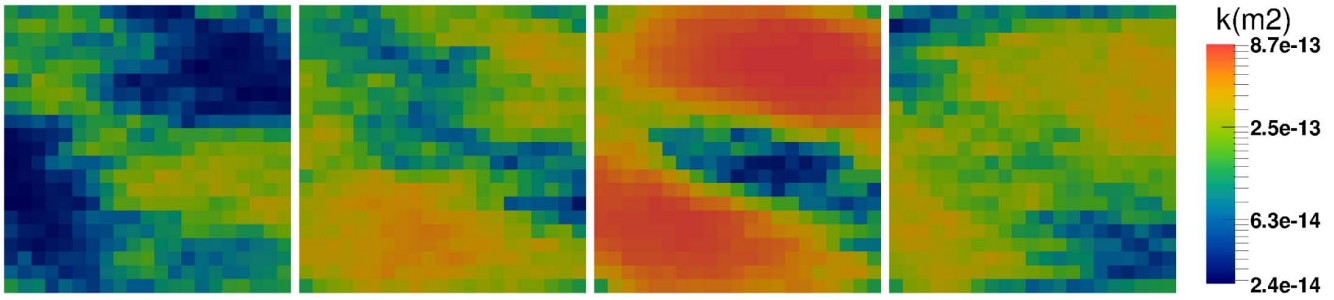

Figure 8—Four different permeability realizations from the ensemble of 1,000 members used in the 2D numerical experiments.

The objective function used for the robust optimization experiments is the expected NPV calculated over the 50 realizations. Fig. 9 illustrates the evolution of the mean NPV through the optimization process for the different simulation models. The same coarsening ratios and initial starting strategy has been used as the deterministic case. The fine scale IMPES model achieves the highest objective function values followed by the i-MSFV 7x7 model and the i-MSFV 3x3 model. Though the five-spot model is relatively small it is reassuring that, irrespective of the different models (fine scale or i-MSFV) used, very similar objective function values have been achieved when geological uncertainties are accounted for.

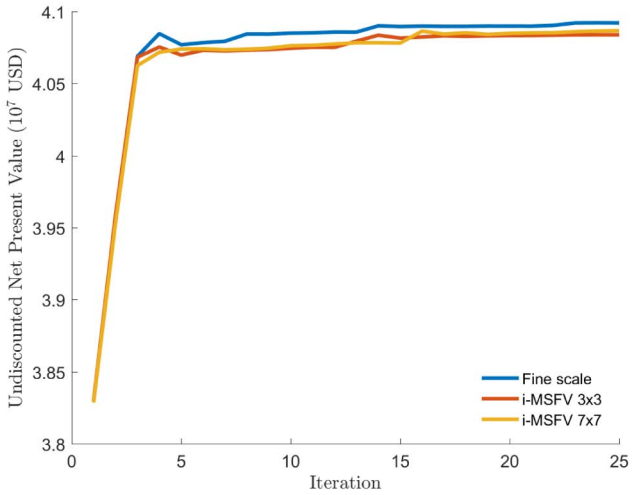

Figure 9—Comparison of the mean objective function value for the three different models, IMPES (blue), i-MSFV 7x7(orange) and i-MSFV 3x3(red)

Fig. 10 is a comparison of the optimal control strategies for two different models, fine scale IMPES and i-MSFV 3x3. The optimal control strategies achieved after robust optimization are quite different from the strategies achieved for deterministic optimization which could be the impact of geological uncertainties, the correspondingly different basis functions and impact of coarsening ratio on the different realizations. A-priori determination of the impact of these factors on the results is non-trivial and is probably model as well as problem dependent.

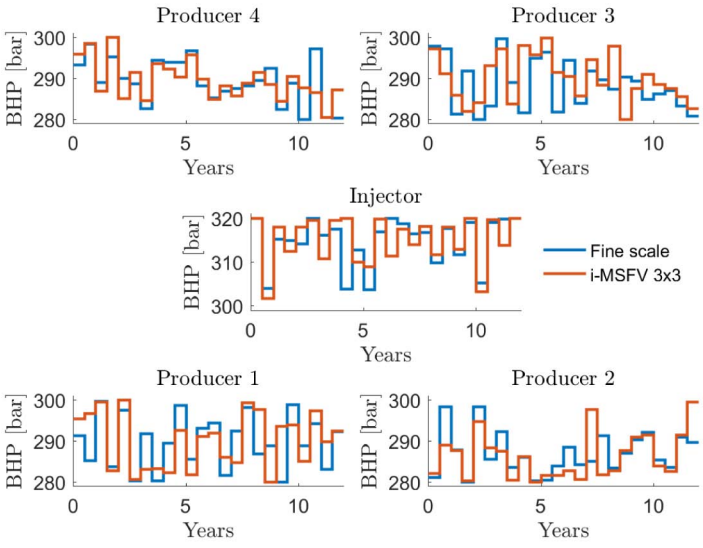

Figure 10—Comparison of the controls that generated the highest NPV

Computational Efficiency. Table 3 provides a comparison of the computational efficiency and speedup gained for the different models used for the experiments. We use the linear solver time to measure the speed up. This accounts for all computations performed by the i-MSFV solution strategy, i.e solution of the coarse system plus fine-scale smoothing. Note that, although the construction of basis function adds an overhead to the total simulation time (Tene et al. 2015), we highlight that in our experiments basis functions are only built once. Also, it is well-known that the linear system solution is the most time-consuming part in reservoir simulation framework.

Table 3—Comparison of the computational effort and average number of smoothing steps for the different i-MSFV cases

Simulation strategy	Time for linear solver (sec)	Number of smoothing steps
IMPES 21×21	4	
i-MSFV 7×7	<1	1
i-MSFV 3×3	<1	2

An approximately factor 4 speedup can be achieved for this relatively small five-spot model. The average number of smoothing steps throughout the optimization is approximately similar, irrespective of the coarsening ratio used which is model and problem dependent. The tolerances of the residual for the MS solution and the smoothing steps are the same for all cases. In order to understand and validate the efficiency of the proposed framework a larger model is used below.

Kanaal Reservoir Model

A second example is considered to illustrate the effectiveness of our proposed workflow. We use a 99 × 99 2D model of with grid blocks of 10 × 10 × 5 m. Thus we have approx. 10,000 grid blocks in this model compared to the 441 grid blocks in the five-spot model. The geological description used in this model has been inspired from a typical channelized North Sea reservoir. The channels (Kanaal in Dutch) are set in a sandy shale background with permeabilities ranging from 10-50 mD. The channels have permeabilities ranging from 250-700mD with constant porosities of 20%. This reservoir is developed using a line drive well configuration with 3 injection wells and 6 production wells as illustrated in Fig. 11. The fluid properties of this reservoir are given in Table 4.

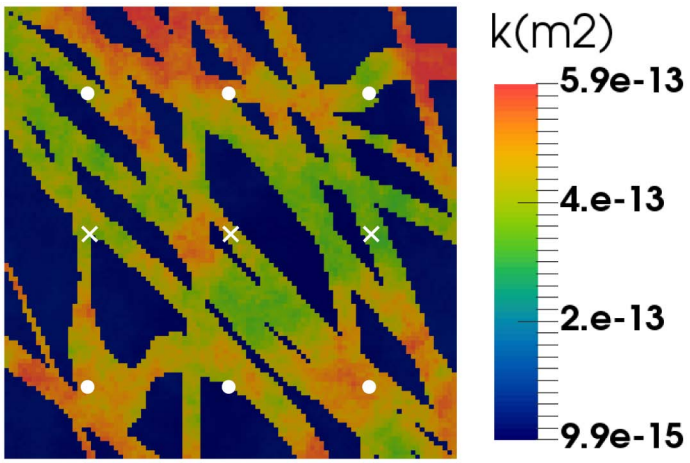

Figure 11—Illustration of the well configuration used for the Kanaal reservoir model with injectors in the middle denoted by X

Table 4—Fluid properties for the Kanaal reservoir model

Property	Value	Unit
Oil dynamic viscosity (μ_o)	2×10^{-3}	Pa s
Water dynamic viscosity (μ_w)	1.0×10^{-3}	Pa s
End-point relative permeability, oil (k_{row})	0.9	-
End-point relative permeability, water (k_{rw})	0.8	-
Corey exponent, oil (N_o)	2.0	-
Corey exponent, water (N_w)	2.0	-
Residual-oil saturation (S_{or} = 0.2)	0.2	-
Connate-water saturation (S_wc)	0.0	-

An ensemble of 50 geological realizations has been created using geological modeling software (Schlumberger 2016) to be used for the robust optimization experiments. Each of the realizations has been constrained to well logs from 4 exploration wells which were generated from a base case model. This base case model does not form part of the ensemble of model realizations. An illustration of a subset of models is illustrated in Fig. 12. The life cycle period for this reservoir is 12 years. We allow the controls, i.e. the bottomhole pressures in all wells, to be manipulated once every 6 months, i.e. 24 we have control time steps. Thus for the 9 wells we optimize a total of 9×24 = 216 controls. The values of the bottomhole pressures are bounded for the production wells between a minimum value of 280 bar and a maximum value of 300 Bar. The injection well pressures are bounded between a minimum value of 300 bar and maximum value of 320 bar.

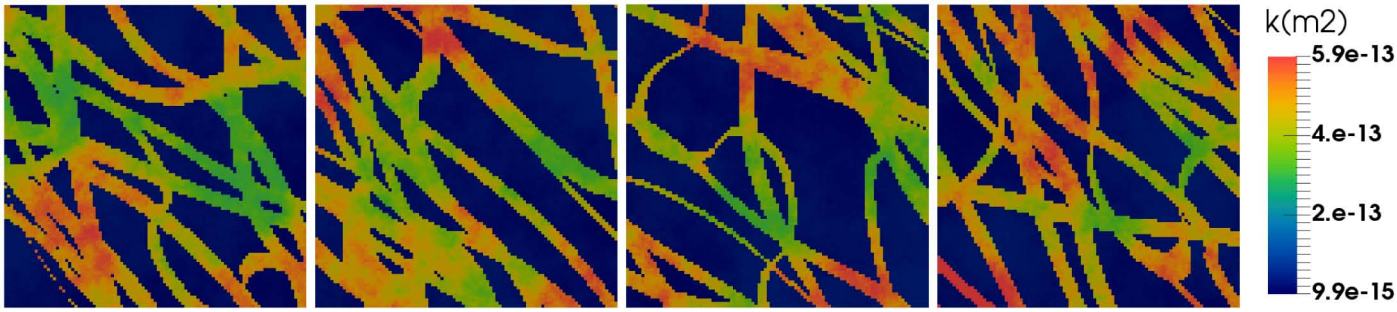

Figure 12—Four different permeabilty realizations from an ensemble of 100 members

Robust Life-cycle Optimization. For this example we focus on robust optimization experiments. The initial control strategy corresponds to the bottomhole pressures on their maximum bound for the injectors, i.e. a constant pressure of 320 bars, and on their minimum bound for the producers, i.e. 280 bars. Different coarsening ratios and their impact on the optimization are investigated. The coarsening ratios for this example are 3×3, 11×11 and 33×33. The fine scale model is 99×99. We observe in Fig. 13 that all the optimization experiments find solutions that achieve an objective function value higher than a reactive control strategy. The economic water cut for the reactive control strategy for the prices considered in this paper is 82%. We also observe from Fig. 13 that different coarsening ratios achieve different optimal mean NPV values with similar trends as observed for the five-spot model. The smaller the coarsening ratio, the higher is the NPV achieved, with the fine scale IMPES solution achieving the highest objective function value. This result is expected because of higher the coarsening ratio, the smaller is the model in terms of grid sizes and thus the lower is the accuracy compared to the finer grid models.

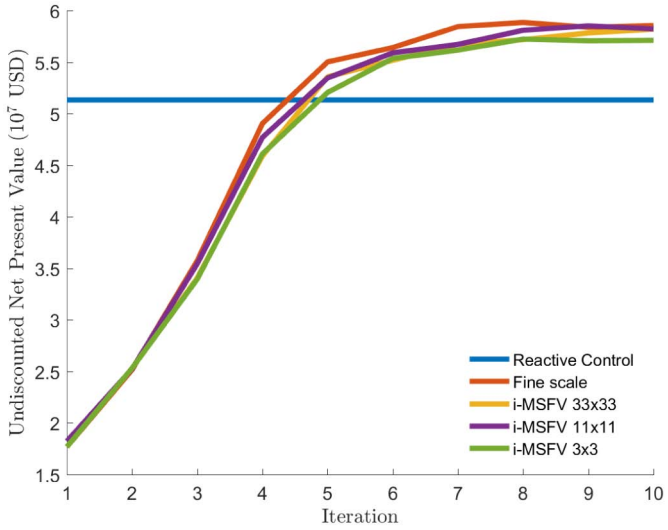

Figure 13—Comparison of objective function value between IMPES and the different i-MSFV models used

Comparison of Optimal Strategies. Fig. 14 is an illustration of the optimal controls for 2 wells for the fine scale IMPES model and the coarser scale i-MSFV 11×11 model. The optimal controls are significantly different from each other with the same trend observed for the other seven wells. The objective function values of the different optimal strategies are very similar to each other even though the strategies are very different which is in accordance with the observation in earliers studies; see, e.g., Jansen et al. (2008). A comparison of the optimal controls for two different i-MSFV models is illustrated in Fig. 15. Once again, we observe that different optimal control strategies achieve very similar objective function values.

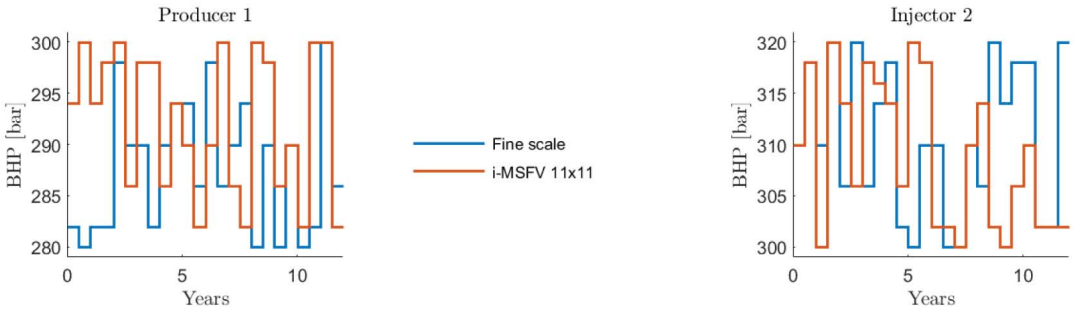

Figure 14—Comparison of the optimal control strategies from IMPES and i-MSFV 11x11 model

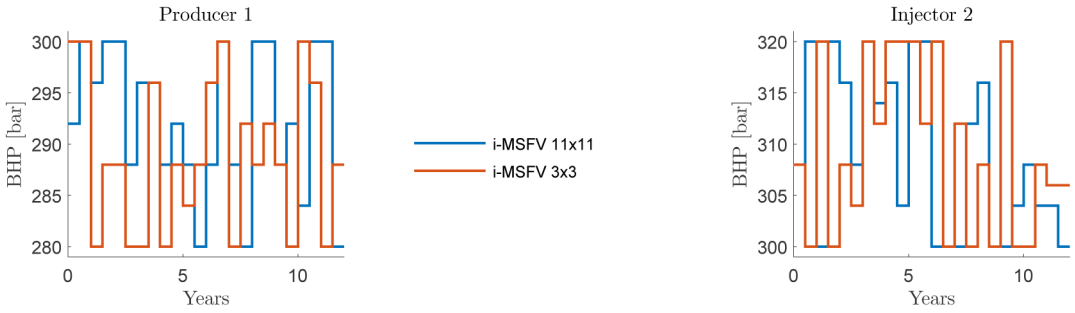

Figure 15—Comparison of the optimal control strategies from i-MSFV 11x11 and i-MSFV 3x3 model

In addition to visually recognising differences in the optimal control strategies we provide in Table 5 a comparison of the optimal volumes of oil and water produced and injected for the different simulation models. We observe an interesting trend in the results. Higher volumes of oil and water are produced in

the i-MSFV models compared to the fine scale IMPES model. Additionally we observe that the higher the coarsening ratio, the higher are the production and injection volumes. We have not yet been able to find a conclusive explanation for these trends.

Table 5—Comparison of optimal produced and injected volumes for the different simulation models

Simulation Strategy	Cumulative Oil Produced	Cumulative Water Produced	Cumulative Water Injected
IMPES 99×99	3.82e5	2.88e5	6.37e5
i-MSFV 33×33	3.87e5	3.09e5	6.97e5
i-MSFV 11×11	3.86e5	3.03e5	6.90e5
i-MSFV 3×3	3.92e5	3.32e5	7.24e5

Computational Efficiency. In this section we compare the computational efficiency and speedup gained for the different coarsening ratios. For the larger Kanaal model an approximately 5 times speedup in computational efficiency is achieved as observed in Table 6. The tolerances of the residual for the MS solution and the smoothing steps are the same for all the cases. We also observe a clear trend in the average number of smoothing steps required for the different coarsening ratios with a higher number of smoothing steps being required for a coarser model.

Table 6—Comparison of the computational effort and average number of smoothing steps for the different i-MSFV cases

Simulation strategy	Speed up for linear solver	Number of smoothing steps
IMPES	1	
i-MSFV 33×33	4.44	5
i-MSFV 11×11	5.69	12
i-MSFV 3×3	4.62	18

Discussion

The multiscale implementation used in this work can be further improved upon to obtain even higher computational efficiency similar to the results reported in Krogstad et al. (2011). The speedup in the computational efficiency reported in Krogstad et al. (2011) was obtained with coarse scale representations for the both the flow and transport equations. In this paper the flow problem is solved at the coarse scale while the transport equation has been solved on the fine scale which improves the accuracy of our results.

Even though no basis function reconstructions were performed in our experiments, and the i-MSFV fine- scale smoothing performed remarkably well, that might not be the case when more complex physics are involved in the simulation model (e.g. gravity effects, capillarity, higher mobility ratios). However, even under more complex scenarioss MS strategies should still deliver considerable speedups given that basis functions need only be built adaptively and infrequently. Also, the employment of different velocity field reconstruction techniques could be necessary in the case that i-MSFV becomes expensive. But again, techniques like those presented by Hajibeygi and Jenny (2011); Jenny et al. (2005) benefit from adaptivity. Furthermore, the implementation of our MS reservoir simulator does not yet capitalize on all potential advantages of MS methods. MS methods are well suited to take full advantage of modern high performance-computing architectures. For instance, the solution of basis functions are embarrassingly parallelizable. Moreover, we expect that the computational advantage will increase for larger-sized reservoir models.

When working with coarse scale models for optimization it is imperative to validate the optimized strategy on the fine scale model to understand and quantify the impact of optimization. Reduced-order or upscaled models, though computationally very efficient, do not always produce similar production

responses compared to the fine scale model. In our approach, because the transport problem is always solved on the fine scale, the optimal strategies need not be validated as is confirmed by the results in this paper. This is an additionally attractive feature of the workflow proposed in this paper. When working with reduced order modeling methods such as POD (van Doren et al. 2006) or TPWL (Cardoso et al. 2010), multiple high-fidelity simulations need to be performed a-priori to develop the reduced order model and afterwards to verify the accuracy of the results. In our workflow we alleviate the need for these expensive pre- and re-computations. As opposed, computation of the basis functions in the MS method is extremely cheap: in the order or seconds to minutes depending on the complexity of the model.

Conclusions

In this paper we presented a computationally efficient multiscale based stochastic optimization (MS-StoSAG) workflow, and applied it to two synthetic test cases. Deterministic and robust optimization experiments were performed to illustrate that significant (10-15%) improvements in objective function values are attainable in a computationally efficient manner. The validation of our results highlights the accuracy of the multiscale forward simulation models. The results from our experiments show that an approximately five times speedup can be achieved with scope for even higher speedups with our proposed workflow. Thus we have shown that a flexible workflow using multiscale forward simulation and stochastic gradients can achieve computationally efficient results of significant practical value.

Acknowledgments

Rafael Moraes' PhD project is sponsored by Petrobras S.A. The authors would like to thank Dr. Hadi Hajibeygi for the discussions related to Multiscale simulation.

References

Aziz, K. and Settari, A. (1979). *Petroleum reservoir simulation*. Applied Science Publishers Ltd., London, U.K.

Cardoso, M. A., Durlofsky, L. J., et al. (2010). Use of reduced-order modeling procedures for production optimization. *SPEJ*, **15**(02):426–435. SPE-119057-PA. http://dx.doi.org/10.2118/119057-PA.

Chen, Y. (2008). *Ensemble-Based Closed-Loop Production Optimization*. PhD thesis, The University of Oklahoma.

Chen, Y., Oliver, D. S., and Zhang, D. (2009). Efficient ensemble-based closed-coop production optimization. *SPEJ*, **14**(04):634–645. SPE-112873-PA. http://dx.doi.org/10.2118/112873-PA.

Chen, Z., Huan, G., and Li, B. (2004). An improved IMPES method for two-phase flow in porous media. *Transport in Porous Media*, **54**(3):361–376. http://dx.doi.org/10.1023/B:TIPM.0000003667.86625.15.

Coats, K. et al. (2003). IMPES stability: The CFL limit. *SPEJ*, **8**(03):291–297. SPE-85956-PA. http://dx.doi.org/10.2118/85956-PA.

Cusini, M., Lukyanov, A. A., Natvig, J., and Hajibeygi, H. (2015). Constrained pressure residual multiscale (CPR-MS) method for fully implicit simulation of multiphase flow in porous media. *Journal of Computational Physics*, **299**:472–486. http://dx.doi.org/10.1016Zj.jcp.2015.07.019.

Do, S. T. and Reynolds, A. C. (2013). Theoretical connections between optimization algorithms based on an approximate gradient. *Computational Geosciences*, **17**(6):959–973. http://dx.doi.org/10.1007/s10596-013-9368-9.

Fonseca, R., Leeuwenburgh, O., Van den Hof, P., Jansen, J.-D., et al. (2014a). Improving the ensemble-optimization method through covariance-matrix adaptation. *SPEJ*, **20**(01):155–168. SPE-163657-PA. http://dx.doi.org/10.2118/163657-PA.

Fonseca, R., Stordal, A., Leeuwenburgh, O., Van den Hof, P., and Jansen, J. (2014b). Robust ensemble-based multi-objective optimization. In ECMOR XIV-14th European conference on the mathematics of oil recovery. Sicily, Italy, 8-11 September 2014. https://www.scopus.com/inward/record.uri?eid=2-s2.0-84908153652&partnerID=40&md5=b7532d2661cbd061688178ec4c05b1dd.

Fonseca, R.-M., Chen, B., Jansen, J. D., and Reynolds, A. (2016). A stochastic simplex approximate gradient (StoSAG) for optimization under uncertainty. *International Journal for Numerical Methods in Engineering*. http://dx.doi.org/10.1002/nme.5342.

Fonseca, R. M., Kahrobaei, S. S., Van Gastel, L. J. T., Leeuwenburgh, O., and Jansen, J. D. (2015). Quantification of the impact of ensemble size on the quality of an ensemble gradient using principles of hypothesis testing. *In SPE Reservoir*

Simulation Symposium. Society of Petroleum Engineers. Texas, USA, 23-25 February 2015. SPE-173236-MS. http://dx.doi.org/10.2118/173236-MS.

Hajibeygi, H., Bonfigli, G., Hesse, M. A., and Jenny, P. (2008). Iterative multiscale finite-volume method. *Journal of Computational Physics*, **227**(19):8604–8621. http://dx.doi.org/10.1016Zj.jcp.2008.06.013.

Hajibeygi, H. and Jenny, P. (2011). Adaptive iterative multiscale finite volume method. *Journal of Computational Physics*, **230**(3):628–643. http://dx.doi.org/10.1016/j.jcp.2010.10.009.

Hajibeygi, H., Lee, S. H., Lunati, I., et al. (2012). Accurate and efficient simulation of multiphase flow in a heterogeneous reservoir with error estimate and control in the multiscale finite-volume framework. *SPEJ*, **17**(04):1—071. SPE-141954-PA. http://dx.doi.org/10.2118/141954-PA.

Hou, T. Y. and Wu, X.-H. (1997). A multiscale finite element method for elliptic problems in composite materials and porous media. *Journal of computational physics*, **134**(1):169–189. http://dx.doi.org/10.1006/jcph.1997.5682.

Jansen, J. D. (2011). Adjoint-based optimization of multi-phase flow through porous media-a review. *Computers & Fluids*, **46**(1):40–51. http://dx.doi.org/10.1016/j.compfluid.2010.09.039.

Jansen, J. D. (2013). A simple algorithm to generate small geostatistical ensembles for subsurface flow simulation. *Research note*. Dept. of Geoscience and Engineering, Delft University of Technology, The Netherlands. http://resolver.tudelft.nl/uuid:6000459e-a0cb-40d1-843b-81650053e093.

Jansen, J.-D., Bosgra, O. H., and Van den Hof, P. M. (2008). Model-based control of multiphase flow in subsurface oil reservoirs. *Journal of Process Control*, **18**(9):846–855. http://dx.doi.org/10.1016/j.jprocont.2008.06.011.

Jansen, J. D. and Durlofsky, L. J. (2016). Use of reduced-order models in well control optimization. *Optimization and Engineering*, pages 1–28. http://dx.doi.org/10.1007/s11081-016-9313-6.

Jenny, P., Lee, S., and Tchelepi, H. (2005). Adaptive multiscale finite-volume method for multiphase flow and transport in porous media. *Multiscale Modeling & Simulation*, **3**(1):50–64. http://dx.doi.org/10.1137/030600795.

Jenny, P., Lee, S. H., and Tchelepi, H. A. (2003). Multi-scale finite-volume method for elliptic problems in subsurface flow simulation. *Journal of Computational Physics*, **187**(1):47–67. http://dx.doi.org/10.1016/S0021-9991(03)00075-5.

Jenny, P. and Lunati, I. (2009). Modeling complex wells with the multi-scale finite-volume method. *Journal of Computational Physics*, **228**(3):687–702. http://dx.doi.org/10.1016/j.jcp.2008.09.026.

Kozlova, A., Li, Z., Natvig, J. R., Watanabe, S., Zhou, Y., Bratvedt, K., and Lee, S. (2015). A real-field multiscale black-oil reservoir simulator. In SPE Reservoir Simulation Symposium. Society of Petroleum Engineers. Texas, USA, 23-25 February 2015. SPE-173226-MS. http://dx.doi.org/10.2118/173226-MS.

Kozlova, A., Walsh, D., Chittireddy, S., Li, Z., Natvig, J., Watanabe, S., and Bratvedt, K. (2016). A hybrid approach to parallel multiscale reservoir simulator. In ECMOR XIV-15th European Conference on the Mathematics of Oil Recovery. Amsterdam, The Netherlands, 29 August-1 September 2016. http://dx.doi.org/10.3997/2214-4609.201601889.

Krogstad, S., Hauge, V. L., and Gulbransen, A. (2011). Adjoint multiscale mixed finite elements. *SPEJ*, **16**(01):162—171. SPE-119112-PA. http://dx.doi.org/10.2118/119112-PA.

Lie, K., Møyner, O., Natvig, J., Kozlova, A., Bratvedt, K., Watanabe, S., and Li, Z. (2016). Successful application of multiscale methods in a real reservoir simulator environment. In ECMOR XIV-15th European Conference on the Mathematics of Oil Recovery. Amsterdam, The Netherlands, 29 August-1 September 2016. http://dx.doi.org/10.3997/2214-4609.201601893.

Lie, K.-A., Krogstad, S., Ligaarden, I. S., Natvig, J. R., Nilsen, H. M., and Skaflestad, B. (2012). Open-source matlab implementation of consistent discretisations on complex grids. *Computational Geosciences*, **16**(2):297—322. http://dx.doi.org/10.1007/s10596-011-9244-4.

Moraes, R., Rodrigues, J., Hajibeygi, H., and Jansen, J. D. (2016). Multiscale gradient computation for subsurface flow models. *Journal of Computational Physics*, (submitted 13 July 2016).

Nocedal, J. and Wright, S. (2006). *Numerical optimization*. Springer Science & Business Media.

Saad, Y. (1994). ILUT: A dual threshold incomplete LU factorization. *Numerical linear algebra with applications*, **1**(4):387—402. http://dx.doi.org/10.1002/nla.1680010405.

Schlumberger (2016). *Petrel*. http://www.software.slb.com/products/petrel (accessed 21 November 2016).

Spall, J. C. (1992). Multivariate stochastic approximation using a simultaneous perturbation gradient approximation. *IEEE transactions on automatic control*, **37**(3):332—341. http://dx.doi.org/10.1109/9.119632.

Stordal, A. S., Szklarz, S. P., and Leeuwenburgh, O. (2016). A theoretical look at ensemble-based optimization in reservoir management. *Mathematical Geosciences*, **48**(4):399—417. http://dx.doi.org/10.1007/s11004-015-9598-6.

Tene, M., Wang, Y., and Hajibeygi, H. (2015). Adaptive algebraic multiscale solver for compressible flow in heterogeneous porous media. *Journal of Computational Physics*, **300**:679–694. http://dx.doi.org/10.1016/j.jcp.2015.08.009.

van Doren, J. F., Markovinovic, R., and Jansen, J.-D. (2006). Reduced-order optimal control of water flooding using proper orthogonal decomposition. *Computational Geosciences*, **10**(1):137–158. http://dx.doi.org/10.1007/s10596-005-9014-2.

Van Essen, G., Zandvliet, M., Van den Hof, P., Bosgra, O., Jansen, J.-D., et al. (2009). Robust waterflooding optimization of multiple geological scenarios. *SPEJ*, **14**(01):202–210. SPE-102913-PA. http://dx.doi.org/10.2118/102913-PA.

Wang, Y., Hajibeygi, H., and Tchelepi, H. A. (2014). Algebraic multiscale solver for flow in heterogeneous porous media. *Journal of Computational Physics*, **259**:284–303. http://dx.doi.org/10.1016/ji.jcp.2013.11.024.

Zhou, H. and Tchelepi, H. A. (2012). Two-stage algebraic multiscale linear solver for highly heterogeneous reservoir models. *SPEJ*, **17**(02):523–539. SPE-141473-PA. http://dx.doi.org/10.2118/141473-PA.

Appendix

Comparison of optimization performance between FIM and IMPES

There exists many different numerical schemes used in reservoir simulators. Fully Implicit (FIM) solution schemes form the most commonly used technique. Other numerical schemes such as Implicit Pressure Explicit Saturation (IMPES), though computationally attractive, can in some cases result in less accurate results, especially in case of strong coupling between pressures and saturations as often occurs in near-well bore regions. At the other hand, small saturation time steps, which are a necessity in the IMPES scheme to maintain numerical stability, result in lower numerical diffusion which typically increases the accuracy of the results (Aziz and Settari 1979). In the examples considered in this paper the same solution accuracy was achieveable with IMPES and FIM. In order to compare results from coarse scale simulation models it is imperative to have a reference fine scale solution. We test the impact of using FIM and IMPES in an optimization context as is illustrated in Fig. 16.

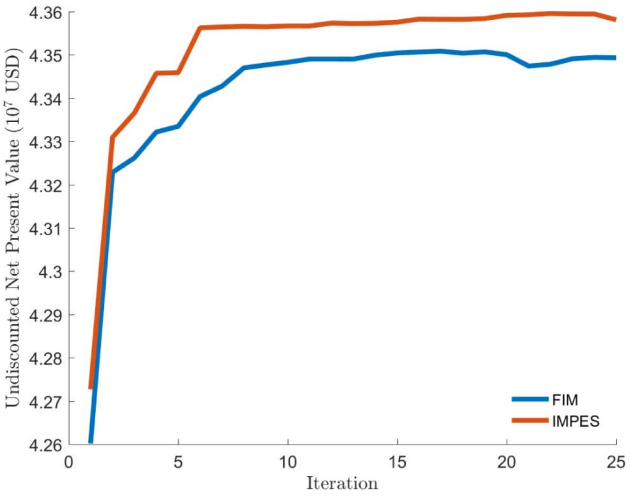

Figure 16—Comparison of the optimization performance between FIM and IMPES

The optimal objective function value achieved when using the IMPES scheme is higher than the optimal objective function values achieved with FIM. We reason this to be due to the well known numerical diffusion errors present in the FIM formulation. These errors result in faster water breakthough and thus larger volumes of water being injected and produced. The optimization also highlights that the optimal control strategies illustrated in Fig. 17 are quite different. Higher volumes of water are injected and produced which will have a negative impact on the objective function used in this paper.

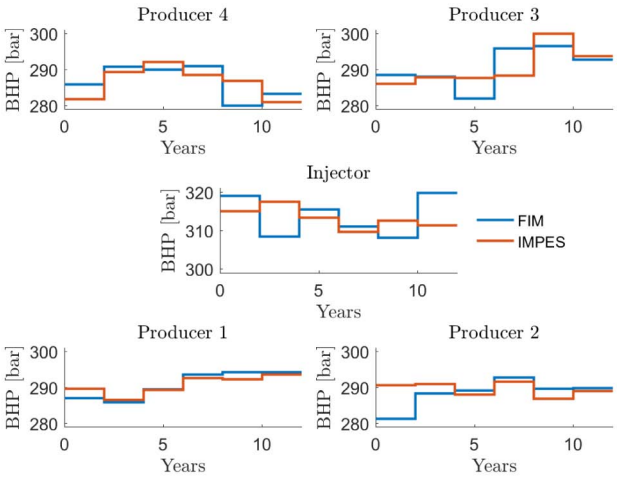

Figure 17—Comparison of the optimal control strategies from FIM and IMPES scheme on fine scale model